AIP Advances

All optical writing and current-driven shifting of bits in ferrimagnetic strips: A micromagnetic study

Cite as: AIP Advances **13**, 015120 (2023); https://doi.org/10.1063/9.0000516
Submitted: 03 October 2022 • Accepted: 04 November 2022 • Published Online: 19 January 2023

Víctor Raposo and Eduardo Martínez

All optical writing and current-driven shifting of bits in ferrimagnetic strips: A micromagnetic study

Cite as: AIP Advances 13, 015120 (2023); doi: 10.1063/9.0000516
Submitted: 3 October 2022 • Accepted: 4 November 2022 •
Published Online: 19 January 2023

Víctor Raposo[a] and Eduardo Martínez

AFFILIATIONS

Departamento de Física Aplicada, Universidad de Salamanca, Plaza de los Caídos S/N, Salamanca 37008, Spain

Note: This paper was presented at the 67th Annual Conference on Magnetism and Magnetic Materials.
[a]**Author to whom correspondence should be addressed:** victor@usal.es

ABSTRACT

Nucleation of domains and domain walls by means of ultrashort laser pulses, and their current-driven shifting along a ferrimagnetic strip with high perpendicular magnetic anisotropy on top of a heavy metal, are both explored here by means of advanced micromagnetic modeling. Our results indicate that these systems are ideal candidates to develop high-density and high-efficient domain wall-based memory devices where the information is coded in series of bits in the form of perpendicular *up* and *down* domains flanked by chiral domain walls.

I. INTRODUCTION

A magnetic shift register like the racetrack[1,2] is a recording device consisting of a ferromagnetic strip where series of bits are coded in the form of magnetic domains flanked by domain walls (DWs). It requires three operations: writing, shifting and reading. It has been shown that ultrathin ferromagnetic (FM) strips on top of a heavy metal (HM) are promising platforms to develop such shift registers. These HM/FM stacks present a strong perpendicular magnetic anisotropy, and the DWs separating *up* and *down* domains adopt a homochiral configuration due to the Dzyaloshinskii–Moriya Interaction (DMI).[3] By injection of current pulses along the HM, a vertical spin polarized current is induced, and the chiral DWs in the FM layer are efficiently driven by means of the spin orbit torque (SOT).[4] These *up* and *down* domains represent the basic elements of binary information, either bit "1" and bit "0", and such coded information can be locally read using a magnetic tunnel junction (MTJ) on top of a local part of the FM/HM stack. Although nowadays the current-driven shifting and reading operations are well established, the preliminary writing operation, that is the local nucleation of a reversed domain, remains elusive. Conventionally, such nucleation has been achieved by injecting a current pulse along an orthogonal bit line. This pulse generates a magnetic Oersted field which locally reverses the magnetization in the FM strip.[5] However, the Oersted field that nucleates a new domain can also annihilate already shifted DWs[5] in the FM strip, and consequently also destroys the stored information. To solve this issue, solutions based on modifying the strip geometry,[6,7] adding more voltage terminals,[8,9] locally modifying the perpendicular anisotropy[10] or using a 'double bit line'[5] configuration have been proposed. However, these solutions still require external attachments and a more intricate multilayer design which complicates the fabrication.

Instead of ferromagnetic strips, ferrimagnetic alloys (FiMs), formed by Rare-Earth (RE) and Transition-Metal (TM) antiferromagnetically coupled sublattices, constitute nowadays the most promising platform to develop the next generation for ultrafast DW-based spintronics devices. These alloys combine the advantages of ferromagnetic and antiferromagnetic materials, and their properties can be easily manipulated by tuning the relative composition of the RE and TM.[11,12] For instance, except at the magnetization compensation point, they present a finite magnetization which can be detected with the same techniques as done in ferromagnets. At the same time, the negligible magnetostatic interaction in these FiMs makes them ideal candidates to store information with high density. They have recently raised strong interest owing to their ultrafast magneto-optical switching properties,[13–15] and the possibility to drive series of domain-walls with high speed under current pulses

due to SOTs when the FiM is on top of a HM.[11,12] Indeed, ultrashort laser pulses with fs duration can reverse the local magnetization of the FiM sample, and on the other hand, it has been demonstrated that high DW velocities of ~1 km/s can be achieved close to the temperature of the angular momentum compensation.[16] These two observations suggest that ultrafast and highly efficient shift registers could be designed based on FiM/HM where the writing is optically carried out by laser pulses, and the shifting is performed by current pulses along the HM.

We have developed an advanced micromagnetic model to explore both the local all-optical switching under ultrashort laser pulses with duration of a few fs[17] in extended FiM thin-films, and the current-driven DW dynamics along FiM/HM stacks.[16] Here, we combine both phenomena (ultrafast all-optical switching and the current-driven DW motion) to explore the possibilities of FiM/HM stacks to develop a shift register combining laser-induced writing and current-driven shifting operations. A proper selection of the fluence and duration of the laser pulse results in a reversed domain flanked by two homochiral domain walls, which are subsequently driven along the FiM strip upon injection of current pulses along the HM. In the rest of this work, we will describe the details of the micromagnetic model and how it can be used to infer the potential of these FiM/HM stacks to develop a DW-based memory device. The ultrafast laser-induced local nucleation of a reversed domain involves an ultrafast rise of the local temperature of the FiM, and the written bit is only stabilized once the temperature recovers its initial room temperature value prior to the laser pulse injection. This after-pulse thermal relaxation takes place at the ns scale, and therefore, it imposes a restriction on writing speed, before the injection of the following nanosecond current pulse along the HM. Our work also demonstrates that any sequence of bits can be written and shifted along these FiM/HM stacks, which make these systems ideal platforms for the next generation of DW based recording devices.

II. MICROMAGNETIC MODEL

A typical FiM/HM stack on top of a Si wafer is considered in the present study. The FiM strip is a GdFeCo alloy composed of the two sublattices, the Transition Metal (TM:CoFe) and the Rare Earth (RE:Gd), which are antiferromagnetically coupled to each other. It lies on the xy plane (see Fig. 1(a)), and its length along the longitudinal x-axis is $\ell = 1.5\mu m$. Its cross section in the yz-plane is $w \times t_{FiM} = 200 \times 6\text{nm}^2$. Figure 1(a) shows the FiM/MH stack and the location of the laser. Starting from an initial uniform state of the FiM with the spins of the two sublattices antiparallel to each other along the easy axis z, a linear polarized laser pulse is applied, and the irradiated sample absorbs energy from the laser pulse. The laser spot is assumed to have both spatial $(\eta = \eta(\vec{r}) = \exp\left[4\ln(2)\left[(x-x_C)^2 + (y-y_C)^2\right]/(2r_0)^2\right]$, where (x_C, y_C) indicate the location of the laser spot, and $r_0 = 0.5\mu m$ is the full width at half maximum of the laser spot), and temporal $(\xi = \xi(t) = \exp\left[4\ln(2)\left[(t-t_0)^2\right]/\left(\tau_L^2\right)\right]$, with $\tau_L = 50$ fs being the pulse length) Gaussian profiles. The absorbed power density can be expressed as $P(r,t) = Q\eta(\vec{r})\xi(t)$, where Q is the maximum value of the absorbed power density reached at $t = t_0$, just below the center of the laser spot.

The thermal evolution of the sample caused by laser pulses is described by the Two Temperatures Model (TTM)[18] in terms of the electron $(T_e = T_e(\vec{r},t))$ and the lattice $(T_l = T_l(\vec{r},t))$ temperatures:

$$C_e\frac{\partial T_e}{\partial t} = -k_e\nabla^2 T_e - g_{el}(T_e - T_l) + P(r,t) - C_e\frac{(T_e - T_R)}{\tau_D} \quad (1)$$

$$C_l\frac{\partial T_l}{\partial t} = -g_{el}(T_l - T_e) \quad (2)$$

where $C_e = 1.8\times10^5\frac{\text{J}}{\text{m}^3\cdot\text{K}}$ and $C_l = 3.8\times10^6\frac{\text{J}}{\text{m}^3\cdot\text{K}}$ denote the specific heat of electrons and lattice subsystems, respectively. $k_e = 91\frac{\text{W}}{\text{m}\cdot\text{K}}$ is the electronic thermal conductivity. $g_{el} = 7\times10^{17}\text{W}/\left(\text{m}^3\cdot\text{K}\right)$ is a coupling parameter between the electron and lattice subsystems, and τ_D is the characteristic heat diffusion time to the Si substrate and the surrounding media. The value of $\tau_D = 1.7$ ns was calculated considering that the whole HM/FiM stack is placed on top of a silicon substrate with a thin silicon oxide layer. COMSOL Multiphysics was used[19] to study the thermal evolution of the system, and we extracted the characteristic time τ_D governing the thermal relaxation of the FiM to the substrate temperature.

Taking into account the temperature evolution of the sample, the magnetization dynamics of each sublattice (i : RE, TM) is governed by the extended Landau-Lifshitz-Bloch Eq. (eLLB),[17]

$$\frac{\partial\vec{m}_i}{\partial t} = -\gamma'_{0i}(\vec{m}_i + \vec{H}_i) - \frac{\gamma'_{0i}\alpha_i^{\perp}}{m_i^2}\vec{m}_i\times\left[\vec{m}_i\times(\vec{H}_i + \vec{\xi}_i^{\perp})\right] + \frac{\gamma'_{0i}\alpha_i^{\parallel}}{m_i^2}(\vec{m}_i\cdot\vec{H}_i)\vec{m}_i + \vec{\xi}_i^{\parallel} + \tau_i^{NE} + \vec{\tau}_{SOT,i} \quad (3)$$

where $\vec{m}_i = \vec{m}_i(\vec{r},t)$ is the local magnetic moment of each sublattice, and $\vec{H}_i = \vec{H}_i(\vec{r},t)$ is the corresponding effective field, which includes all the usual micromagnetic contributions (inter- and intra-lattice exchange, anisotropy, magnetostatic and interfacial DMI). $\alpha_i^{\parallel}$ and $\alpha_i^{\perp}$ are the longitudinal and perpendicular damping parameters, and $\vec{\xi}_i^{\parallel}$ and $\vec{\xi}_i^{\perp}$ are the longitudinal and perpendicular stochastic thermal fields. $\vec{\tau}_i^{NE}$ is an additional torque that considers the non-equilibrium magnetic moment exchange between sublattices. Finally, the last term in Eq. (1), $\vec{\tau}_{SOT,i} = \gamma'_{0i}H^0_{SH,i}(\vec{m}_i\times\vec{\sigma})$, represents the spin orbit torque acting on the FiM strip as due to the injection of current pulses along the HM underneath $(\vec{J} = J(t)\vec{u}_x)$. $\vec{\sigma} = \vec{u}_z\times\vec{u}_x$ is the polarization factor of the spin current, and $H^0_{SH,i}(t) = \frac{\hbar\theta_{SH,i}J(t)}{2|e|\mu_0 M_{si}t_{FiM}}$ represents the Slonczewski-Like-SOT magnitude, where $\theta_{SH,i} = 0.1$ is the spin Hall angle, $|e|$ is the electric charge, μ_0 is the free space permeability and M_{si} is the spontaneous magnetization of each sublattice. Equation (3) is numerically solved as coupled to Eqs. (1) and (2) using a finite difference scheme, where the FiM is discretized in elementary cells with dimensions of $\Delta x = \Delta y = 1$ nm and $\Delta z = t_{FiM}$. The spontaneous magnetizations at zero temperature of each sublattice are $M_{s,TM}(0) = 0.41$ MA/m and $M_{s,RE}(0) = 0.55$ MA/m. The exchange stiffness constants are $A_{ex,TM} = 3.2$ pJ/m and $A_{ex,RE} = 0.19$ pJ/m. The anisotropy constants are $K_{u,TM} = 1.87$ MJ/m^3 and $K_{u,RE} = 0.62$ MJ/m^3. The DMI constant is $D = 0.12$ mJ/m^2. Damping parameter is $\alpha_{RE} = \alpha_{TM} = 0.02$. All micromagnetic details and the rest of material parameters can be found in Ref. 17.

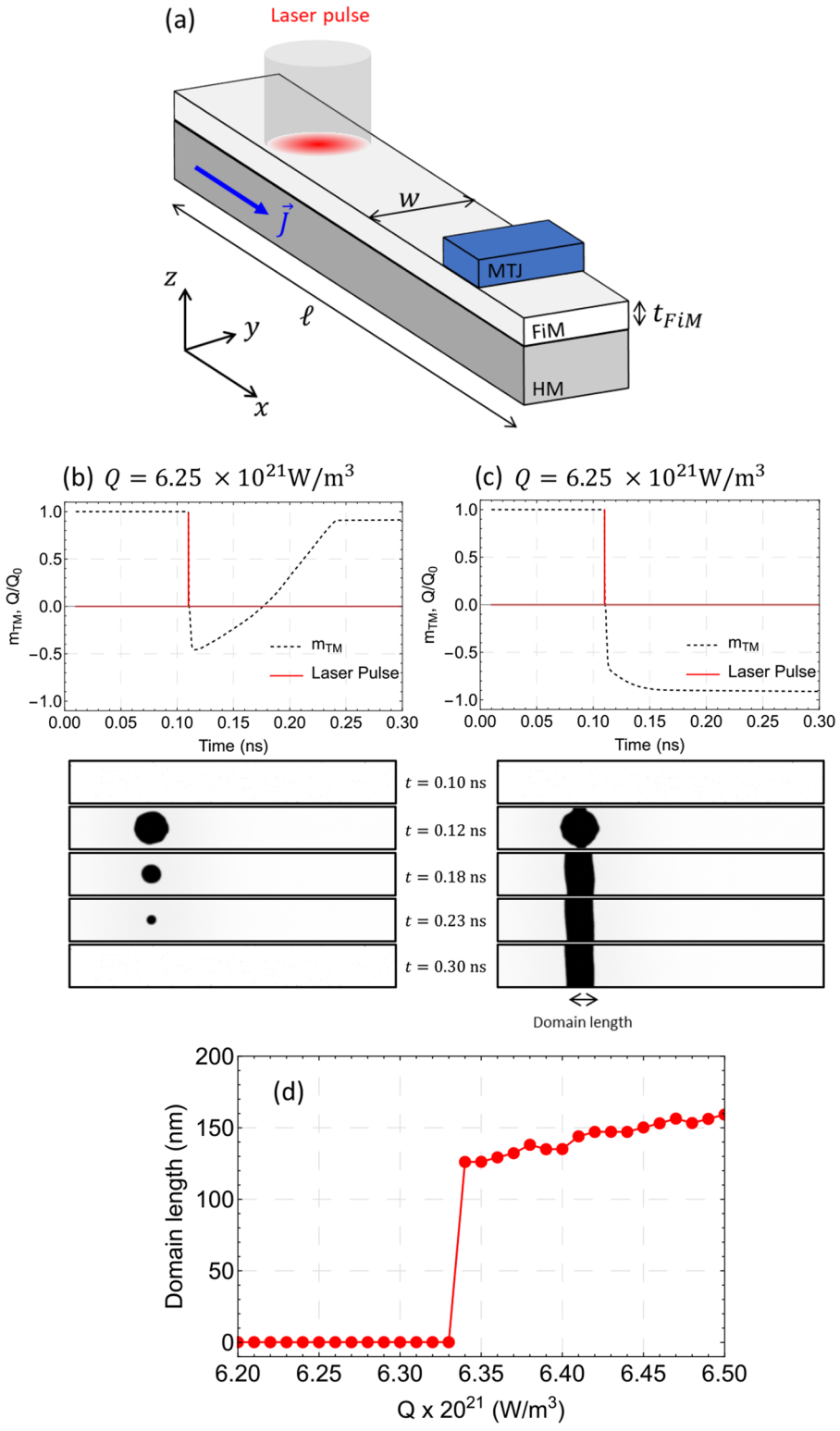

FIG. 1. (a) Scheme of the HM/FiM shift register with the indication of the laser beam. (b) and (c) depict the temporal evolution of the laser pulse and the resulting magnetic state in the TM for $Q = 6.25 \times 10^{21}$ W/m^3 and $Q = 6.35 \times 10^{21}$ W/m^3 power densities respectively. (d) Reverse domain length as a function of Q.

III. RESULTS AND DISCUSSION

We firstly analyze the minimum power density (Q) of the laser pulse needed to nucleate or locally reverse the initial magnetization of the FiM. In the initial state both sublattices are uniformly magnetized along the z-axis and antiparallel to each other: TM is initially *up*, and therefore, the RE is *down*, as shown in the snapshots of Fig. 1(b). A $\tau_L = 50$ fs long laser pulse with $Q = 6.25 \times 10^{21}$ W/m^3 nucleates a transient circular reversed domain in the FiM. However, this domain does not fill the full width of the FiM strip and it finally collapses (Fig. 1(b)). If the laser power exceeds a threshold, the magnetization of the FiM is locally reversed after the laser pulse as shown in Fig. 1(c) for $Q = 6.35 \times 10^{21}$ W/m^3. The reversed domain is flanked by two DWs (*up-down* and *down-up* from left to right in the TM, and the opposite in the RE sublattice), and its length along the x-axis increases with Q as indicated in Fig. 1(d). The stabilization of the laser-induced reversed domain is completed around 200 ps after the pulse, which is more than one order of magnitude faster than conventional nucleation method using a bit line.[5,20] Moreover, its length is ~125 nm, which determines the size of each bit, results in an information density of ~8 bits/μm.

Once the laser-induced nucleation conditions are established, the next step is to explore the shifting of the written information from the nucleation region along the FiM register. As mentioned before, this can be done with high efficiency in HM/FiM stacks by injecting current pulses along the HM ($J = J(t)$), which drives both DWs at both sides of the reversed domain with the same velocity. We have studied the DW velocity in the same HM/FiM as a function of the injected current density J considering the effect of the Joule heating. The power density introduced in the system due to the current pulse enters in the TTM as $P(r,t) = J^2(t)/\gamma$, where γ is the electrical conductivity of the HM. The time traces of three representative current pulses are shown in Fig. 2(a). The corresponding temperature evolution in the sample and the DW displacements are shown in Figs. 2(b) and 2(c) respectively. Note that the Joule heating only increments the temperature of the sample a few degrees above room temperature during the current pulse, and the temperature relaxes again to its initial value once the current pulse is switched off. As expected, the temperature reached by the sample at the end of the current pulse increases with the pulse amplitude (J) and with the length (τ_J) of the electrical pulses. The post-pulse relaxation time towards room temperature increases with J and τ_J, and, therefore, in order reduce the time between consecutive current pulses, working with low-amplitude and short pulses is preferred. The average DW velocity as a function of the amplitude of the current pulse is shown in Fig. 2(d) for three different pulse durations (τ_J). Such average DW velocity was computed as the total displacement divided by the pulse length, $\Delta x_{DW}/\tau_J$. Note also that due to the strong antiferromagnetic coupling these DWs do not depict inertia,[16] and they stop once the current pulse is switched off.

We have now all the ingredients to combine the laser-induced nucleation (writing) and the current-driven shifting of the information along the FiM register. We use laser pulses with $\tau_L = 50$ fs and $Q = 6.35 \times 10^{21}$ W/m^3 to write a reversed *down* domain when needed. Note that these laser inputs determine the length of the reversed domain to ~125 nm, and therefore, the amplitude (J) and the duration (τ_J) of the injected current pulses have to be adapted to this bit size. According to the study presented in Fig. 2, this can be done current pulses of $J = 1$ TA/m^2 and $\tau_J = 0.25$ ns or $J = 0.5$ TA/m^2 and $\tau_J = 0.5$ ns. For these current pulses, the DWs are displaced a distance matching the bit size (125 nm). As an example, we show how to write and shift the following sequence of bits "01101000", where *up* state in the TM sublattice corresponds to the logical "1" and *down* state to the "0". After each laser pulse, we let the system to recover its initial thermal equilibrium state during a 0.2 ns before applying the shifting current pulse. We add a delay of 10 ns between current pulses to ensure the cooling down of the temperature to room temperature. Laser and current pulses

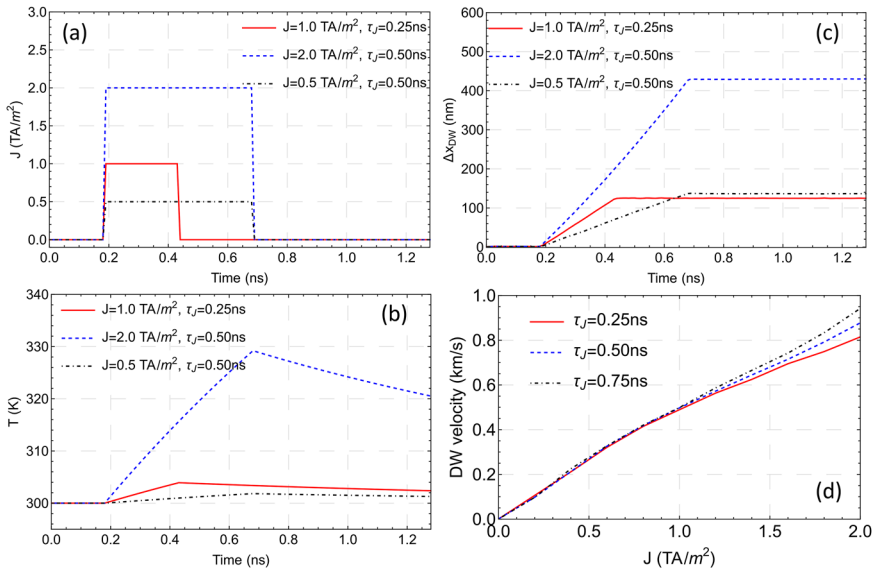

FIG. 2. (a) Time traces of three different current pulses injected along the HM. (b) and (c) show the temporal evolution of the temperature and the DW displacement for the same current pulses respectively. (d) Averaged DW velocity as function of the amplitude (J) of the current pulse for three different pulse durations (τ_J).

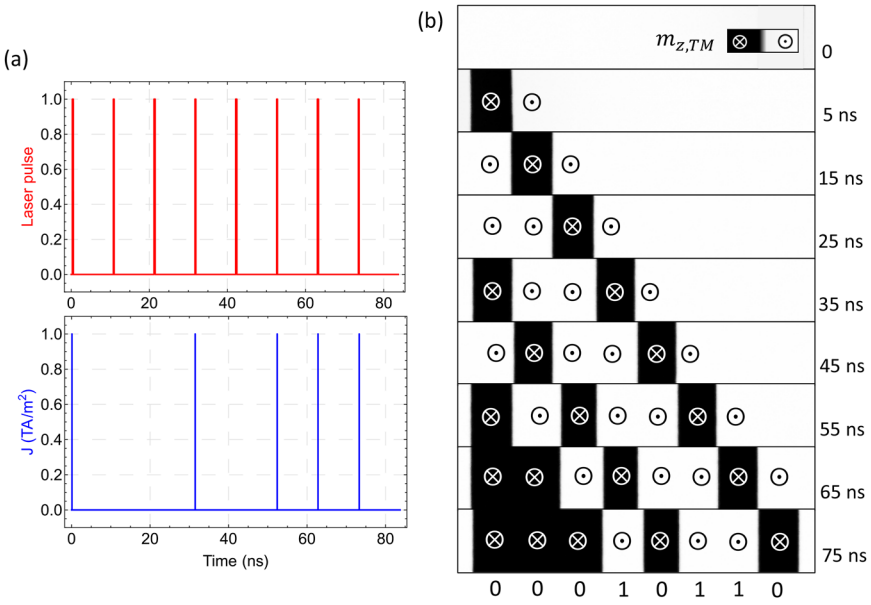

FIG. 3. (a) Time traces of the laser pulses (τ_L = 50 fs and $Q = 6.35 \times 10^{21}$ W/m^3) and the current pulses (J = 1 TA/m^2 and τ_J = 0.25 ns) injected along the HM to write and shift a bit sequence of "01101000" along the HM/FiM register. (b) Micromagnetic snapshots of the resulting magnetization state at different instants of time.

needed to write the "01101000" sequence are shown in Figs. 3(a) and 3(b) respectively. The resulting snapshots at different instants of time are shown in Fig. 3(c). As can be observed, the bit sequence is correctly written and placed in each bit location, without destroying the previous data when writing and moving the following bits. The procedure is reliable, and for all the data series we tried (not shown in the figures) the information was correctly written and shifted.

IV. CONCLUSIONS

We have presented a full micromagnetic model which allows us to combine the local optical switching of a ferrimagnetic alloy under ultrashort linear polarized laser pulses with current-driven domain wall motion as due to the injection of current pulses along a heavy metal under the ferrimagnetic strip. With this model, we have explored the possibility of designing a shift register where information is written in the form of up and down domains by ultrashort laser pulses, which later are driven away by the injection of current pulses due to spin orbit torque. Using typical material parameters and working under realistic conditions, our results suggest that these systems can store information at high density (~8 bits/μm) which can be shifted at high velocity (1 km/s) with low energy consumption. All these features make these systems ideal candidates to develop DW-based shift registers. The main speed limitation of the device is caused by the time needed to wait between pulses to cool down the sample to room temperature (~1 – 10 ns). This waiting time is imposed by the thermal characteristics of the substrate and could be improved by the use of substrates with higher thermal conductivity.

ACKNOWLEDGMENTS

This work was supported by Grant MAT2017-87072-C4-1-P funded by Ministerio de Ciencia e Innovacion and No. PID2020-20117024GB-C41 funded by MCIN/AEI/10.13039/501100011033, both from the Spanish government, Projects No. SA299P18 and No. SA114P20 from Consejeria de Educacion of Junta de Castilla y León, and project MagnEFi, Grant Agreement No. 860060, (H2020-MSCA-ITN-2019) funded by the European Commission.

AUTHOR DECLARATIONS

Conflict of Interest

The authors have no conflicts to disclose.

Author Contributions

Víctor Raposo: Conceptualization (equal); Data curation (equal); Formal analysis (equal); Funding acquisition (equal); Investigation (equal); Methodology (equal); Project administration (equal); Resources (equal); Software (equal); Supervision (equal); Validation (equal); Visualization (equal); Writing – original draft (equal); Writing – review & editing (equal). **Eduardo Martínez**: Conceptualization (equal); Data curation (equal); Formal analysis (equal); Funding acquisition (equal); Investigation (equal); Methodology (equal); Project administration (equal); Resources (equal); Software (equal); Supervision (equal); Validation (equal); Visualization (equal); Writing – original draft (equal); Writing – review & editing (equal).

DATA AVAILABILITY

The data that support the findings of this study are available from the corresponding author upon reasonable request.

REFERENCES

[1] S. S. P. Parkin, M. Hayashi, and L. Thomas, Science **320**, 190 (2008).
[2] S. Parkin and S.-H. Yang, Nat. Nanotechnol. **10**, 195 (2015).
[3] S. Emori, U. Bauer, S.-M. Ahn, E. Martinez, and G. S. D. Beach, Nat. Mater. **12**, 611 (2013).
[4] K.-S. Ryu, L. Thomas, S.-H. Yang, and S. Parkin, Nat. Nanotechnol. **8**, 527 (2013).
[5] O. Alejos, V. Raposo, L. Sanchez-Tejerina, and E. Martinez, Sci. Rep. **7**, 11909 (2017).
[6] S. F. Zhang, W. L. Gan, J. Kwon, F. L. Luo, G. J. Lim, J. B. Wang, and W. S. Lew, Sci. Rep. **6**, 24804 (2016).
[7] D. Osuna Ruiz, O. Alejos, V. Raposo, and E. Martínez, Appl. Phys. Lett. **121**, 102403 (2022).
[8] J. Nan, Y. Zhang, Z. Zhang, K. Zhang, Z. Zheng, G. Wang, X. Zhang, J. O. Klein, D. Ravelosona, Y. Zhang, and W. Zhao, IEEE Trans. Magn. **55**, 9100204 (2019).
[9] Z. Luo, W. Liao, Y. Yang, C. Zhu, and Y. Wu, Appl. Phys. Lett. **111**, 162404 (2017).
[10] T. P. Dao, M. Müller, Z. Luo, M. Baumgartner, A. Hrabec, L. J. Heyderman, and P. Gambardella, Nano Lett. **19**, 5930 (2019).
[11] L. Caretta, M. Mann, F. Büttner, K. Ueda, B. Pfau, C. M. Günther, P. Hessing, A. Churikova, C. Klose, M. Schneider, D. Engel, C. Marcus, D. Bono, K. Bagschik, S. Eisebitt, and G. S. D. Beach, Nat. Nanotechnol. **13**, 1154 (2018).
[12] S. A. Siddiqui, J. Han, J. T. Finley, C. A. Ross, and L. Liu, Phys. Rev. Lett. **121**, 57701 (2018).
[13] A. V. Kimel and M. Li, Nat. Rev. Mater. **4**, 189 (2019).
[14] C. S. Davies, J. H. Mentink, A. V. Kimel, T. Rasing, and A. Kirilyuk, J. Magn. Magn. Mater. **563**, 169851 (2022).
[15] T. A. Ostler, J. Barker, R. F. L. Evans, R. W. Chantrell, U. Atxitia, O. Chubykalo-Fesenko, S. El Moussaoui, L. Le Guyader, E. Mengotti, L. J. Heyderman, F. Nolting, A. Tsukamoto, A. Itoh, D. Afanasiev, B. A. Ivanov, A. M. Kalashnikova, K. Vahaplar, J. Mentink, A. Kirilyuk, T. Rasing, and A. V. Kimel, Nat. Commun. **3**, 666 (2012).
[16] E. Martínez, V. Raposo, and Ó. Alejos, J. Magn. Magn. Mater. **491**, 165545 (2019).
[17] V. Raposo, F. García-Sánchez, U. Atxitia, and E. Martínez, Phys. Rev. B **105**, 104432 (2022).
[18] K. Vahaplar, A. M. Kalashnikova, A. V. Kimel, S. Gerlach, D. Hinzke, U. Nowak, R. Chantrell, A. Tsukamoto, A. Itoh, A. Kirilyuk, and T. Rasing, Phys. Rev. B **85**, 104402 (2012).
[19] COMSOL AB, COMSOL Multiphysics v. 5.3a, COMSOL AB, Stockholm, Sweden, 2021, see www.comsol.com.
[20] J. L. Prieto, M. Muñoz, and E. Martínez, Phys. Rev. B **83**, 104425 (2011).